Single-Molecule Dynamics Reveal an Altered Conformation for the Autoinhibitory Domain of Plasma Membrane Ca^{2+}-ATPase Bound to Oxidatively Modified Calmodulin†

Kenneth D. Osborn,‡ Ryan K. Bartlett,§,|| Abhijit Mandal,‡ Asma Zaidi,⊥ Ramona J. Bieber Urbauer,§,# Jeffrey L. Urbauer,§,# Nadya Galeva,△ Todd D. Williams,△ and Carey K. Johnson*,‡

Departments of Chemistry, Molecular Biosciences, and Pharmacology and Toxicology and Mass Spectrometry Laboratory, University of Kansas, Lawrence, Kansas 66045

Received June 8, 2004; Revised Manuscript Received August 5, 2004

ABSTRACT: We used single-molecule polarization modulation methods to investigate the activation of the plasma membrane Ca^{2+}-ATPase (PMCA) by oxidized calmodulin (CaM). Oxidative modification of methionine residues of CaM to their corresponding sulfoxides is known to inhibit the ability of CaM to activate PMCA. Single-molecule polarization methods were used to measure the orientational mobility of fluorescently labeled oxidized CaM bound to PMCA. We previously identified two distinct populations of PMCA−CaM complexes characterized by high and low orientational mobilities, with the low-mobility population appearing at a subsaturating Ca^{2+} concentration [Osborn, K. D., et al. (2004) *Biophys. J. 87*, 1892−1899]. We proposed that the high-mobility population corresponds to PMCA−CaM complexes with a dissociated (and mobile) autoinhibitory domain, whereas the low-mobility population corresponds to PMCA−CaM complexes where the autoinhibitory domain is not dissociated and therefore the enzyme is not active. In the present experiments, performed with PMCA complexed with oxidatively modified CaM at a saturating Ca^{2+} concentration, we found a large population of molecules with an orientationally immobile autoinhibitory domain. In contrast, native CaM bound to PMCA was characterized almost entirely by the more orientationally mobile population at a similar Ca^{2+} concentration. The addition of 1 mM ATP to complexes of oxidized CaM with PMCA reduced but did not abolish the low-mobility population. These results indicate that the decline in the ability of oxidized CaM to activate PMCA results at least in part from its reduced ability to induce conformational changes in PMCA that result in dissociation of the autoinhibitory domain after CaM binding.

Calmodulin (CaM)[1] is a small, water-soluble, Ca^{2+}-signaling protein found in all eukaryotic cells and involved in a variety of signaling pathways (*1*−*3*). With a structure that consists of two globular domains connected by a central linker region, CaM is able to bind four Ca^{2+} ions through two EF-hand binding motifs in each domain. Upon Ca^{2+} binding, each globular domain exposes a hydrophobic cleft, allowing CaM to recognize and bind a wide variety of protein targets (*4*, *5*). Among these is the plasma membrane Ca^{2+}-ATPase (PMCA) (*6*), a transmembrane Ca^{2+} pump that plays an important role in the maintenance of the intracellular Ca^{2+} concentration. The hydrolysis of ATP at the nucleotide-binding site provides the driving force for Ca^{2+} transport across the plasma membrane. The activity of PMCA is self-regulated by an autoinhibitory domain, which is located near the C-terminal end of the protein and serves also as a CaM binding domain (*7*, *8*). In the inactive enzyme, this domain is believed to associate with the active site containing the nucleotide and phosphorylation domains of the enzyme, thus blocking its ability to bind or utilize ATP (*8*−*10*). CaM binding to the autoinhibitory domain is believed to induce structural changes in the CaM binding domain, triggering dissociation of the autoinhibitory domain from sites near the catalytic core of the enzyme, removing self-inhibition of the enzyme and resulting in severalfold stimulation of PMCA activity (*7*, *8*, *10*).

Oxidative modifications in proteins involved in Ca^{2+} regulatory pathways have been linked to biological aging and a multitude of age-related diseases associated with a decline of the ability of cells to restore baseline Ca^{2+} levels following cell stimulation (reviewed in ref *11*). CaM isolated

† This work was supported by NIH Grants R01 GM58715, NIH AG17996, and NIH P01 AG12993.

* Address correspondence to this author. Phone: 785-864-4219. Fax: 785-864-5396. E-mail: ckjohnson@ku.edu.

‡ Department of Chemistry, University of Kansas.

§ Department of Molecular Biosciences, University of Kansas.

|| Present address: Department of Molecular Physiology and Biophysics, Vanderbilt University Medical Center, Nashville, TN 37232.

⊥ Department of Pharmacology and Toxicology, University of Kansas.

Present address: Department of Biochemistry and Molecular Biology, University of Georgia, Athens, GA 30602.

△ Mass Spectrometry Laboratory, University of Kansas.

[1] Abbreviations: CaM, calmodulin; CaM_{ox}; oxidized calmodulin; CaM-TMR; calmodulin fluorescently labeled with tetramethylrhodamine; EDTA, ethylenediaminetetraacetic acid; EGTA, ethylene glycol bis(2-aminoethyl ether)-*N*,*N*,*N*′,*N*′-tetraacetic acid; ESI-MS, electrospray ionization mass spectrometry; HEPES, *N*-(2-hydroxyethyl)-piperazine-*N*′-2-ethanesulfonic acid; PMCA, plasma membrane Ca^{2+}-ATPase; P_i, inorganic phosphate; TMR, tetramethylrhodamine-5-maleimide.

10.1021/bi048806p CCC: $27.50
Published on Web 09/18/2004

from senescent rat brains showed a progressive decline in its ability to stimulate PMCA activity (*12*). In vitro studies of CaM oxidized by H_2O_2 showed a 30-fold decrease in the affinity of oxidized CaM for Ca^{2+} (*13*). More recent work has shown that oxidized CaM (CaM_{ox}) binds to the PMCA in a nonproductive manner that does not result in PMCA activation (*14*). Oxidation of CaM in vivo has been suggested to serve as a metabolic regulatory mechanism to help to maintain cellular viability under conditions of oxidative stress through the suppression of metabolic and other ATP-utilizing transport processes within the cell (*15*).

Single-molecule spectroscopic methods provide researchers with new tools to study intrinsically heterogeneous systems such as proteins (*16*−*19*). One of the advantages of single-molecule fluorescence methods is the ability to characterize the distribution of structural and functional properties that are hidden by the ensemble averaging inherent in conventional bulk studies. The resolution of these heterogeneities is necessary for the full understanding of structural and dynamic features underlying complex biomolecular processes.

Several optical methods can be implemented at the single-molecule level (*18*−*20*). One of these is single-molecule polarization modulation spectroscopy, which samples the orientational dynamics of single molecules (*21*−*27*). We recently applied single-molecule polarization modulation spectroscopy to investigate the orientational mobility of CaM bound to the autoinhibitory domain of PMCA (*27*, *28*). By continuously varying the orientation of the polarization exciting the sample, the reorientational mobility of the fluorescently labeled CaM bound to the autoinhibitory domain of PMCA can be monitored. Previous results suggested that the orientational mobility of CaM bound to the autoinhibitory domain is correlated to the activity of PMCA (*28*). At a saturating Ca^{2+} concentration (25 μM), an orientationally mobile population of PMCA−CaM was observed. At a lower Ca^{2+} concentration (0.15 μM), however, a population of PMCA−CaM complexes with a low orientational mobility appeared, revealing an intermediate state in the binding and activation of the PMCA by CaM at low Ca^{2+} levels. We attributed this state to CaM bound to the autoinhibitory domain without releasing it from the nucleotide-binding site, so that the pump remains inactive (*28*).

In the present paper, single-molecule polarization modulation spectroscopy has been extended to investigate the mechanistic origin of the nonproductive binding of oxidized CaM to the PMCA. Whereas PMCA−CaM complexes displayed a high orientational mobility at a saturating Ca^{2+} concentration, we find that CaM_{ox} bound to PMCA leads to a large population of orientationally less mobile CaM_{ox} molecules. We also find a large orientationally immobile population of CaM_{ox} for PMCA−CaM_{ox} complexes in the presence of 1 mM ATP. In contrast, our previous results showed that, in normal PMCA−CaM complexes, the presence of ATP resulted in an exclusively orientationally mobile population, consistent with a dissociated autoinhibitory domain and an active enzyme (*28*). Thus, binding of CaM_{ox} to the autoinhibitory domain is insufficient in itself to fully activate the enzyme. This result is consistent with the previous suggestion that CaM_{ox} binds to PMCA in a nonproductive manner that does not lead to enzyme activation (*14*). Our findings suggest that the loss in activation of PMCA results from a reduced ability of CaM_{ox} to induce release of the autoinhibitory domain.

MATERIALS AND METHODS

Materials. The sample for single-molecule measurements was prepared in a standard 10 mM HEPES buffer (pH 7.4) with 0.1 M KCl, 1 mM $MgCl_2$, and 0.214 mM $CaCl_2$, yielding a final concentration of 1 mM free Mg^{2+} and 0.1 mM free Ca^{2+} in solution as calculated with a computer program (*29*) taking into account the composition of the PMCA storage buffer added to the final sample. Low Ca^{2+} buffers were made by addition of 10 mM EGTA and appropriate adjustments in the added $MgCl_2$ and $CaCl_2$ to yield the desired free ion concentrations. The pH was adjusted to 7.4 after addition of EGTA. All reagents used were purchased from Sigma-Aldrich, St. Louis, MO.

Binding of CaM labeled with tetramethylrhodamine to PMCA was carried out in the dark at 4 °C for at least 30 min or at room temperature for 15 min. For samples containing ATP, the nucleotide was added immediately after the binding of CaM to PMCA and prior to mixing with the agarose gel (Sigma, type VIIA). Samples were mixed with agarose gel held slightly above the gelling temperature to yield a final gel concentration of 2.2%. This mixture was placed on a clean, dry coverslip held over a cold block to facilitate rapid setting of the gel. Once the gel was set, a clean coverslip was placed on top of the gel to minimize drying of the sample during the experiments.

Calmodulin Mutagenesis, Expression, Purification, and Fluorescence Labeling. The gene encoding wild-type chicken CaM was amplified by PCR using pEX1-CaM as the template. To facilitate cloning into pBluescript II SK (±) (Stratagene), a *Kpn*I site, along with an *Nco*I site, was added at the 5′ end of the gene. At the 3′ end of the gene, the native stop codon, TGA, was changed to TAA, and a *Bam*HI restriction site was also added. The sequence of the cloned gene was confirmed by DNA sequencing. Using this new construct as the template, residue 34 of CaM was mutated from threonine to cysteine by a PCR method previously described (*30*). The mutation was confirmed by DNA sequencing and then cloned into pET-15b (Novagen). CaM overexpression and purification were performed as previously described (*31*). T34C-CaM was fluorescently labeled with TMR (Molecular Probes, Eugene, OR) following standard protocols provided by the supplier, as previously described (*28*). CaM labeled in this fashion is denoted CaM-TMR. Labeled protein was stored at −80 °C immediately after dialysis. Samples were removed from cold storage immediately prior to experimental measurements.

Plasma Membrane Ca^{2+}-ATPase Purification and Activity Assays. PMCA for single-molecule measurements was purified from freshly drawn human blood with a CaM−Sepharose column (Amersham Biosciences) and reconstituted into micelles following previously described procedures (*32*). The storage buffer for the PMCA contained 10 mM HEPES adjusted to pH 7.4, 120 mM NaCl, 2 mM EDTA, 2 mM $MgCl_2$, 0.5 mM $CaCl_2$, 0.4 mg/mL $C_{12}E_8$, and 5% (v/v) glycerol.

Activity measurements of CaM, T34C-CaM, and CaM-TMR were carried out with PMCA in porcine erythrocyte ghost membranes (*33*). PMCA activity assays were per-

formed as previously described (*28*) with 0.05 mg/mL porcine erythrocyte ghosts in a buffer containing 100 mM HEPES (pH 7.5), 0.1 M KCl, 5 mM $MgCl_2$, 0.1 mM EGTA, 0.44 mM $CaCl_2$, 5 mM ATP, and 4 μM calcium ionophore A23187 (Sigma-Aldrich, St. Louis, MO) and the desired concentration of CaM. After a 5 min preincubation period, the reaction was started by the addition of 1 mM ATP, continued for 20 min at 37 °C, and then stopped by the addition of Malachite Green dye solution (*34*). The contents were made acidic by addition of 19.5% H_2SO_4 and incubated for 45 min, and the absorbance was measured at 660 nm in a microwell plate reader. The PMCA activity was defined as the Ca^{2+}-activated ATP hydrolysis and expressed as micromoles of inorganic phosphate (P_i) liberated per milligram of ghost-membrane vesicle per hour, based on values from a standard curve of the absorbance for various concentrations of free inorganic phosphate. A control assay was performed with free TMR at the same dye concentrations as present with the labeled CaM samples to test for any spectrophotometric interference from the dye. No changes were seen between phosphate standards containing dye and phosphate standards without dye when the absorbance at 660 nm was measured following addition of the Lanzetta reagents (*34*). Calculations of free CaM concentrations for activity assay purposes were carried out as previously described (*31*). The concentration of free Ca^{2+} was calculated as described in ref *29*.

Oxidative Modification of Calmodulin. To oxidize all nine methionines in CaM to methionine sulfoxides, samples were exposed to 100 mM H_2O_2 for 24 h at 25 °C as described previously (*31*). CaM-TMR with TMR covalently attached to cysteine 34 was oxidized after dye labeling. Free TMR was also subjected to 100 mM H_2O_2 as a control, and only a small reduction in overall fluorescence yield was observed, showing that only a small fraction of TMR molecules were oxidized.

Mass Spectrometry. ESI-MS was performed to verify whole protein sample masses and to confirm complete oxidative modification of methionine residues within CaM. The ESI mass spectra in positive mode were acquired on a Q-TOF 2 quadrupole, time-of-flight hybrid instrument (Micromass Ltd., Manchester, U.K.). Parameters for mass spectrometry were the same as previously described (*31*).

Single-Molecule Instrumentation. The single-molecule instrumentation used for these experiments has been described in detail previously (*28*). Briefly, a 543 nm polarized helium−neon laser beam was passed through an electrooptic modulator (M-350, ConOptics) and a quarter waveplate, resulting in a continuously rotating linear excitation-beam polarization at 25 revolutions per second. An excitation filter (D543/10x, Chroma) removed any unwanted excitation wavelengths from the ≤ 1 μW beam, which was then reflected by a dichroic mirror (Q555LP, Chroma) into a 1.3 numerical-aperture objective in an inverted fluorescence microscope (TE300, Nikon). Fluorescence collected by the objective lens was directed through the dichroic mirror and an emission filter (HQ600/80m, Chroma) to an avalanche photodiode (SPCM-AQR-14, Perkin-Elmer Optoelectronics). Single-molecule fluorescence trajectories were analyzed to determine the modulation depth period by period as described in detail elsewhere (*27*).

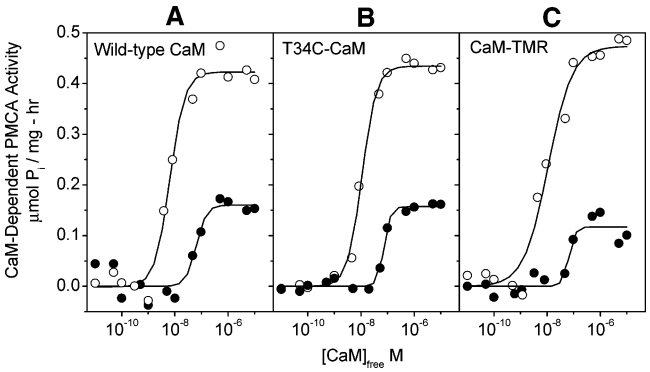

FIGURE 1: CaM-dependent activation of the PMCA by wild-type CaM (A), T34C-CaM (B), and CaM-TMR (C) before (○) and after (●) oxidation of CaM by hydrogen peroxide. ATPase activity was measured at 37 °C with 0.05 mg/mL porcine erythrocyte ghosts. The CaM-stimulated activity was obtained as the difference between activity in the presence of CaM and the average basal activity in the absence of CaM. Average errors in ATPase activity measurements were 6% of indicated values.

RESULTS

Activity of Modified Calmodulin. Previous results showed that oxidation of native CaM with hydrogen peroxide (H_2O_2) decreases its ability to maximally stimulate PMCA (*13*, *31*). Figure 1 shows the activity of PMCA present in porcine ghost membranes with increasing concentrations of CaM. PMCA activity was stimulated by wild-type CaM and wild-type CaM_{ox} (Figure 1A), T34C-CaM and T34C-CaM_{ox} (Figure 1B), and CaM-TMR and CaM_{ox}-TMR (Figure 1C). Values for the measured PMCA activity and apparent CaM affinity are listed in Table 1 for native CaM, T34C-CaM, and CaM-TMR and for the corresponding oxidized CaM species. The results indicate comparable levels of PMCA activation by the wild-type CaM, T34C-CaM, and CaM-TMR, showing that neither the introduction of the T34C mutation nor the TMR dye label alters the properties of CaM as determined by its ability to activate PCMA (Figure 1). By demonstrating that neither the mutation of threonine 34 to cysteine nor the covalent addition of TMR to the mutated cysteine alters the activity of CaM, we can be assured that a biologically representative model is being tested. When PMCA activity was determined in the presence of CaM oxidized with H_2O_2, it was obvious in all three cases that CaM_{ox} does not activate the enzyme to the same extent as the reduced protein. Wild-type CaM_{ox}, T34C-CaM_{ox}, and CaM_{ox}-TMR each show roughly a 60% decrease in V_{max} compared to the native reduced CaM (Table 1). The CaM concentration required for half-maximal activation, $[CaM]_{1/2\,free}$, was substantially increased upon oxidation, from a value of 6−10 nM for wild-type CaM, T34C-CaM, and CaM-TMR to 64−69 nM for the corresponding oxidized species.

Since the protocol for oxidation of the CaM required exposure of the sample to room temperature conditions for 24 h, it was also necessary to determine if such exposure at room temperature leads to any decrease in CaM activity. Parallel exposure of T34C-CaM to the same room temperature conditions (but without exposure to H_2O_2) revealed no discernible loss in activity. Oxidative conditions may also alter the fluorescence properties of the TMR dye. To determine if this is indeed the case, we took the emission spectra of control and oxidized CaM-TMR. The results show

Table 1: CaM Apparent Binding Affinity and Activation of Plasma Membrane Ca-ATPase[a]

CaM sample	$[CaM]_{1/2\ free}$[b] (nM)	$V_{max}(CaM)$[b] (μmol of P_i mg^{-1} h^{-1})	$[CaM_{ox}]_{1/2\ free}$[c] (nM)	$V_{max}(CaM_{ox})$[c] (μmol of P_i mg^{-1} h^{-1})
wild type	6 ± 1	0.42 ± 0.01	64 ± 18	0.16 ± 0.01
T34C-CaM	10 ± 1	0.44 ± 0.01	69 ± 5	0.16 ± 0.01
CaM-TMR	10 ± 3	0.47 ± 0.02	66 ± 16	0.12 ± 0.01

[a] Values obtained from data in Figure 1. $[CaM]_{1/2\ free}$ is the concentration of CaM required for half-maximal activation of the PMCA, and V_{max} is the CaM-dependent activation of the PMCA at saturating CaM concentrations. [b] CaM samples prior to oxidation. [c] CaM samples after exposure to 100 mM H_2O_2 for 24 h.

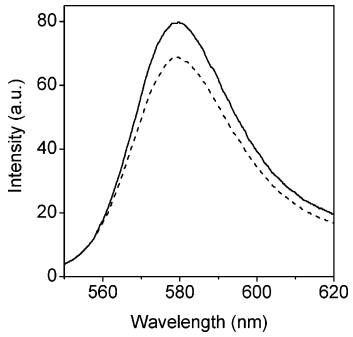

FIGURE 2: Fluorescence spectra of CaM-TMR before (full line) and after (dashed line) oxidation by hydrogen peroxide to generate CaM_{ox}-TMR.

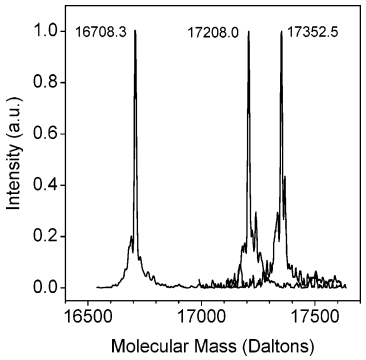

FIGURE 3: ESI mass spectra of T34C-CaM (left curve), CaM-TMR (center), and CaM_{ox}-TMR (right). The uncertainty in the experimentally determined masses is ± 0.8 amu. The predicted masses are 16708.5 for T34C-CaM, 17208.0 for CaM-TMR (with an opened maleimide ring), and 17352.0 for CaM_{ox}-TMR (with an opened maleimide ring). See text for analysis of mass spectra.

a small drop in fluorescence intensity in CaM_{ox}-TMR in comparison to the control. Figure 2 displays the fluorescence spectra of the control and CaM_{ox}-TMR samples, showing a 14% drop in emission intensity but no perceptible shift in fluorescence wavelength or in the shape of the fluorescence spectrum. Since oxidation of dyes results in complete loss of fluorescence ("bleaching"), the fluorescence loss observed in Figure 2 is likely due to oxidation of a small fraction of dye molecules. Because these molecules are not fluorescent, they are invisible in single-molecule experiments and therefore do not contribute to the reported measurements.

Mass Spectrometry of Oxidized Proteins. To verify that there were no other modifications of CaM-TMR upon oxidation by peroxide beyond the conversion of all nine intrinsic methionine residues into methionine sulfoxides, whole-protein ESI-MS was performed on the sample. In addition to the nine methionine residues, it is also possible that the non-native cysteine introduced at site 34 and labeled with an extrinsic dye might offer another potential site of modification by H_2O_2. Figure 3 shows the mass spectra of T34C-CaM, CaM-TMR, and CaM_{ox}-TMR. The observed masses correspond within the resolution of the instrument (± 0.8 amu) with the predicted masses in each case (see Figure 3 caption). The mass observed for CaM_{ox}-TMR shows the presence of nine additional oxygen atoms, consistent with the oxidation of all nine methionine residues as seen in previous work on CaM (*31*). Thus, the mass spectrum indicates that the labeled cysteine residue was not oxidized. A mass difference of 18 amu for both CaM-TMR and CaM_{ox}-TMR can be attributed to a ring opening hydrolysis reaction of the succinimide linkage (*35*) after the reaction of maleimide with the sulfhydryl group of the cysteine. As the level of PMCA activation was nearly the same regardless of labeling by an extrinsic fluorophore, it can be concluded that the ring opening does not affect the function of the CaM.

Anisotropy Decay Measurements. To further check the possible effect of maleimide ring opening on the spectroscopic measurements, we measured the bulk fluorescence anisotropy decay of CaM_{ox}-TMR samples and found rotational correlation times of 0.6 ± 0.1 ns (representing 48% $\pm$ 4% of the anisotropy decay amplitude) and 8 ± 2 ns (representing 52% $\pm$ 4% of the anisotropy decay amplitude). These values are close to those for native CaM-TMR of 0.7 ± 0.1 ns (34% $\pm$ 6% of the anisotropy decay amplitude) and 11 ± 2 ns (66% $\pm$ 6% of the anisotropy decay amplitude) as reported previously (*28*). These measurements permit assessment of the extent of independent mobility of TMR with respect to the protein to which it is attached. For this purpose, the important factor is the relative amplitudes of the fast and slow rotational correlation times. The shorter rotational correlation time for both CaM-TMR and CaM_{ox}-TMR can be assigned to orientational motion of the dye itself, and the longer rotational correlation time represents rotational motion of CaM-TMR or CaM_{ox}-TMR as a whole, showing that the orientational motion of TMR in both cases is partially restricted relative to CaM or CaM_{ox}. Thus we find no decrease in mobility of TMR relative to CaM_{ox}; on the contrary, the mobility of TMR with respect to CaM_{ox} appears if anything to be slightly greater than the mobility of TMR relative to CaM, as shown by the slightly larger relative amplitude of the fast rotational component for CaM_{ox}-TMR. Hence, the increased population of the low-mobility state that we observe for PMCA$-CaM_{ox}$-TMR cannot result from a decrease in the mobility of TMR relative to CaM_{ox}, and therefore reports the mobility of CaM_{ox}-TMR complexed with PMCA.

Single-Molecule Studies. Single-molecule polarization modulation experiments permit measurement of the orientational mobility of the fluorophore (*27*). Modulation depths for native CaM bound to PMCA were determined by single-molecule polarization modulation as described previously

(*28*). In the present studies, a similar strategy was used with CaM_{ox}-TMR added to samples of PMCA, which were then immobilized in a 2.2% agarose gel. Single PMCA−CaM_{ox}-TMR complexes were located by scanning a 10 μm × 10 μm area of the gel with the microscope objective focused several micrometers above the surface of the coverslip. We found previously that CaM-TMR by itself cannot be immobilized in an agarose gel but rather diffuses through the gel (*30*). Thus, single-molecule images observed in a scan of the gel result only from CaM_{ox}-TMR immobilized by binding to PMCA. This was verified by the absence of single-molecule images in the absence of PMCA (*28*). Fluorescence trajectories from PMCA−CaM_{ox}-TMR complexes located in this way were recorded, and the modulation depth was determined by maximum-likelihood analysis as described previously (*27*, *28*). The average modulation depth for each molecule was determined over its fluorescence trajectory.

Single-molecule polarization modulation spectroscopy determines the orientational mobility of molecules on the time scale of the period of modulation of the excitation beam polarization, 40 ms in this case. Fluorophores that rapidly reorient on this time scale explore a range of orientations with respect to the incident polarization. The fluorescence emission of orientationally mobile molecules therefore shows little or no modulation. Immobile molecules, however, show strong modulation in their emission, as the probability of absorbing a photon is related to the relative orientations of the transition dipole of the dye molecule and the orientation of the excitation polarization. The modulation depth is a value between 0 and 1 giving the fraction of the average fluorescence intensity that is modulated over each period of modulation (*27*). Restricted orientational motion results in a modulation depth >0. Orientationally immobile molecules therefore have a high modulation depth. However, unmodulated contributions to the signal (for example, background counts and polarization components along the *z* axis in the focal region) result in measured modulation depths of <1, even for orientationally immobile molecules. These issues have been addressed in greater detail elsewhere (*27*).

Histograms of single-molecule modulation depths for PMCA−CaM_{ox} complexes at a Ca^{2+} concentration of 25 μM are shown in Figure 4. Earlier work has shown that there is only a slight increase in the amount of Ca^{2+} necessary for maximal activation of the PMCA by oxidized CaM (*13*), and the saturating levels used in this experiment are more than sufficient to provide maximal activity of the PMCA−CaM_{ox} complex. For comparison, the previously reported single-molecule modulation depth histograms for complexes of PMCA with native CaM at Ca^{2+} concentrations of 25 and 0.15 μM are also shown (Figure 4A,B) (*28*). With native CaM, single-molecule polarization modulation histograms revealed the presence of a population with a low modulation depth indicating a high orientational mobility at a saturating Ca^{2+} concentration of 25 μM (*28*). We attributed this orientationally mobile population to PMCA−CaM complexes with a dissociated autoinhibitory domain. At a subsaturating Ca^{2+} concentration of 0.15 μM, we observed, in addition to the high-mobility populaton, a populaton of PMCA−CaM complexes with a high modulation depth indicating a reduced orientational mobility (shown in Figure 4B). We hypothesized that this population corresponded to PMCA−CaM complexes where the autoinhibitory domain is not dissociated

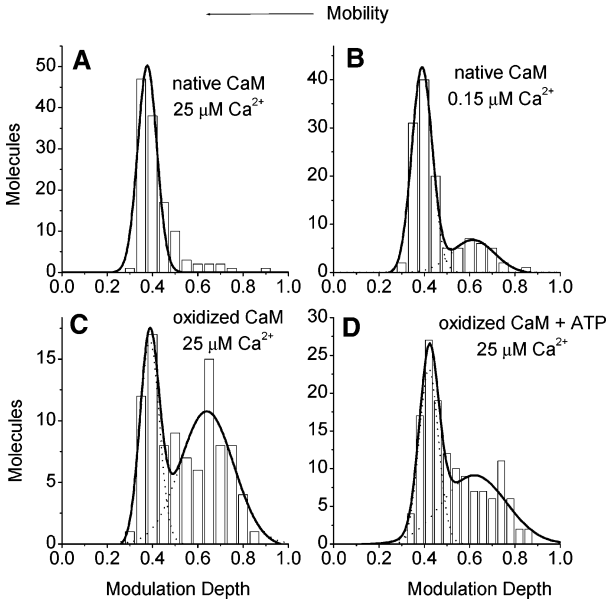

FIGURE 4: Modulation depth histograms for complexes of native PMCA with (A) CaM-TMR at 25 μM Ca^{2+}, (B) CaM-TMR at 0.15 μM Ca^{2+}, (C) CaM_{ox}-TMR at 25 μM Ca^{2+}, and (D) CaM_{ox}-TMR at 25 μM Ca^{2+} in the presence of 1 mM ATP. The histograms show the occurrences of modulation depths for single molecules determined by polarization modulation at 25 Hz. The modulation depth for each molecule was determined from the average modulation depth in the single-molecule polarization modulation fluorescence trajectory. The solid lines show fits to a single Gaussian distribution (A) or a double Gaussian distribution (B−D). The Gaussian fits yield peak positions at modulation depths of 0.38 (panel A), 0.39 and 0.61 (panel B), 0.39 and 0.64 (panel C), and 0.42 and 0.62 (panel D). In panels B−D, the dashed lines show the Gaussian components of the double Gaussian fit. The data in panels A and B were reported previously (*28*) and are shown here for comparison purposes.

(and therefore the PMCA is inactive) even though CaM is bound. The addition of ATP was found to abolish the low-mobility population, even at a subsaturating Ca^{2+} concentration.

The modulation depth histogram for PMCA−CaM_{ox} complexes (Figure 4C), also at a Ca^{2+} concentration of 25 μM, reveals a dramatic increase in the population exhibiting a higher modulation depth (>0.5), indicative of a low orientational mobility of PMCA−CaM_{ox} complexes, in comparison to the same data taken for the native CaM (Figure 4A). The distributions in Figure 4C were fit well by a double Gaussian function, suggesting that the distributions can be described by the presence of two populations of PMCA−CaM_{ox} complexes. In this fit, the width of the distribution for the low mobility state is over twice that of the high mobility state, suggesting a wide range of mobilities in the low-mobility state (Figure 4C).

The modulation depths of single PMCA−CaM_{ox} complexes were also determined in the presence of 1 mM ATP. The presence of ATP allows turnover of PMCA, permitting observation of the effect of conformational changes in PMCA following nucleotide binding and evaluation of the biological relevance of CaM oxidation for PMCA function. The polarization modulation histogram for PMCA−CaM_{ox} in the presence of ATP is shown in Figure 4D. Previous results with native CaM complexed with PMCA in the presence of ATP (*28*) showed that the low-mobility population (modulation depth greater than roughly 0.5) vanished entirely in the

presence of ATP. In contrast, PMCA−CaM_{ox} complexes in the presence of ATP still show a substantial population with low orientational mobility (Figure 4D), suggesting that even though CaM_{ox} binds to PMCA, it suffers a reduced ability to elicit conformational changes in PMCA that couple binding to activation.

To compare distributions, it is useful to compare the fraction of molecules having average modulation depths greater than or less than 0.5 (a value intermediate between the peaks of the low-mobility and high-mobility populations). For native PMCA, the fraction of the population with modulation depth above 0.5 is 0.09 at a Ca^{2+} concentration of 25 μM (Figure 4A). For PMCA−CaM_{ox} complexes, this fraction is 0.60 (Figure 4C). In the presence of ATP, the fraction of the population with modulation depth above 0.5 is 0.53 (Figure 4D), compared to 0.06 for native PMCA−CaM in the presence of ATP (*28*). The decrease by ~50% in the population of the highly mobile state can be compared to a decrease in bulk activity by ~60−75% upon CaM oxidation shown in Figure 1.

DISCUSSION

Oxidative modification of Ca^{2+} regulatory proteins has been implicated in the reduced ability of cells to regulate the intracellular concentration of Ca^{2+} following oxidative stress as well as in biological aging and neurodegenerative diseases such as Alzheimer's disease (refs *11*, *13*, and *36*−*39* and references cited therein). A number of studies have demonstrated conclusively that oxidation of the methionine residues of CaM causes a decrease in its ability to stimulate PMCA (*13*, *14*, *31*). All nine methionine residues in CaM can be oxidized to methionine sulfoxides when the protein is exposed to oxidative conditions. It has been reported that oxidized CaM can still bind to PMCA, but the binding results in a diminished efficiency in activation of PMCA (*14*). Selective mutations of specific methionine residues demonstrated that Met 144 and Met 145 in the carboxy-terminal domain of CaM are responsible for the loss in CaM-stimulated activation of the PMCA by CaM_{ox} (*13*, *31*). The C-terminal domain of CaM exhibits higher Ca^{2+} affinity and tighter binding than the N-terminal domain for most targets, including PMCA (*40*−*45*). However, the structural and dynamic origins by which oxidative modification of CaM leads to loss of PMCA activity are not well understood.

To identify mechanisms involved in the decline in the ability of CaM_{ox} to stimulate PMCA, we carried out single-molecule studies of the orientational mobility of CaM_{ox}-TMR bound to the autoinhibitory/CaM binding domain of PMCA. CaM binding to the autoinhibitory domain is thought to lead to its release from the catalytic regions of the enzyme, allowing PMCA to function. This view is supported by measurements of the rotational correlation time of CaM bound to PMCA at a Ca^{2+} concentration sufficient to saturate all four Ca^{2+} binding sites of CaM (*46*). The measured rotational correlation time of 80 ns, while too long to represent reorientational dynamics of CaM itself, is much too fast to represent reorientation of the PMCA as a whole, suggesting that CaM is bound to a domain that is highly mobile relative to the rest of the PMCA. Recent single-molecule polarization measurements in our laboratory are consistent with this picture (*28*).

Single-molecule methods offer the ability to distinguish inhomogeneity within the population of oxidized CaM bound to the PMCA autoinhibitory domain. This approach is based on the apparent correlation that we observed (*28*) between the orientational mobility of CaM bound to the autoinhibitory domain of PMCA and the activity of PMCA. The modulation depth of PMCA−CaM complexes under saturating Ca^{2+} is low (Figure 4A), consistent with a highly mobile dissociated autoinhibitory domain. In contrast, single-molecule polarization measurements revealed the presence under certain conditions of a fraction of PMCA−CaM complexes having a low orientational mobility. This population was present at a Ca^{2+} concentration of 0.15 μM (Figure 4B) but was absent or minimal at a saturating Ca^{2+} concentration of 25 μM (Figure 4A) or with the addition of ATP. We proposed that the population with a high orientational mobility corresponds to PMCA−CaM complexes with a dissociated autoinhibitory domain, while the population with a low orientational mobility corresponds to PMCA−CaM complexes where the autoinhibitory domain is not dissociated and the pump is therefore inactive (*28*). This interpretation is supported by the results reported in the present studies, which show a large population of orientationally immobile PMCA−CaM_{ox} complexes at a saturating Ca^{2+} concentration, consistent with the decreased activity observed in these complexes.

These results provide insight into the mechanism of the decline in the ability of oxidized CaM to stimulate PMCA. Based on our interpretation of the population with low orientational mobility in terms of PMCA−CaM complexes with a nondissociated autoinhibitory domain, the orientationally immobile population appears to correspond to PMCA−CaM_{ox} complexes with a nondissociated autoinhibitory domain. Thus, although CaM_{ox} can still bind to the autoinhibitory domain of PMCA, binding no longer provides the necessary structural or conformational changes within the PMCA needed for dissociation of the autoinhibitory domain. The addition of ATP reduces but does not abolish the orientationally immobile population of PMCA−CaM_{ox} complexes. In contrast, orientational distributions of native PMCA−CaM complexes showed that in the presence of ATP the low-mobility population is nearly absent, suggesting that structural changes in the course of the enzymatic cycle of PMCA alter the ability of the autoinhibitory domain to associate with the catalytic site (*28*). Large-amplitude structural changes between states with high (E_1) and low (E_2) Ca^{2+} affinity were observed in X-ray (*47*, *48*) and cryo-electron microscopy (*49*) structures of the homologous sarcoplasmic/endoplasmic reticulum Ca^{2+}-ATPase. Such motions in PMCA may generate a conformation where association of the autoinhibitory domain with the catalytic site is inhibited. The presence of a low-mobility population of PMCA−CaM_{ox} complexes, even in the presence of ATP, further indicates that binding of CaM_{ox} may not induce the structural changes necessary for PMCA to function.

Binding of CaM is known to induce an α-helical structure within the binding region in many target proteins (*50*−*54*). The nine methionine residues of CaM play an important role both in stabilizing the open conformation of CaM upon Ca^{2+} binding and in the high affinity of interactions with targets such as PMCA (*55*−*59*). Squier and co-workers demonstrated that whereas Met 144 and Met 145 are not essential for activation of PMCA (*60*), the oxidation of Met 144 and

Met 145 results in at least 50% reduction in the level of enzyme activation (*31*) as a result of incorrect association of the C-terminal domain of CaM with PMCA (*14*).

The present results are consistent with these findings. The modulation depth distributions for complexes of CaM_{ox} with PMCA suggest that the decreased ability of CaM_{ox} to activate PMCA upon binding results from a population of the autoinhibitory domains still associated with the PMCA in an inhibitory manner, even though CaM is bound. This suggests that CaM_{ox} is unable to induce α-helix formation in the autoinhibitory domain upon binding to PMCA. This could result from the altered binding of the C-terminal domain of CaM_{ox} due specifically to oxidation of Met 144 and Met 145 (*31*). The population with low orientational mobility (modulation depth >0.5 in Figure 4) detected for PMCA−CaM_{ox} complexes displays a wide distribution of modulation depths. The large width of the distribution may arise from a range of association states in the CaM-bound autoinhibitory domain and is consistent with the previous suggestion that the nature of the binding by CaM_{ox} is altered within the 30-residue CaM binding region of the PMCA (*14*).

CONCLUSIONS

We demonstrated the use of single-molecule polarization modulation experiments to investigate the mechanism of loss of activation of a target enzyme, PMCA, by oxidatively modified CaM. CaM is central to a range of cellular processes, including energy metabolism and Ca^{2+} signaling. Under conditions of oxidative stress, the formation of CaM_{ox} can therefore have severe consequences for Ca^{2+} regulation and energy utilization. It has been suggested that the susceptibility of the C-terminal methionines (Met 144 and Met 145) to oxidation allows CaM to function as a redox sensor and to downregulate energy metabolism under conditions of oxidative stress (*31*).

Single-molecule modulation depth distributions revealed a large orientationally immobile population of PMCA−CaM_{ox} complexes under saturating Ca^{2+}. In contrast, the modulation depth distributions of complexes of PMCA with native CaM show a predominantly orientationally mobile population, with only a small fraction of molecules belonging to a population with lower orientational mobility. We argued that orientationally mobile PMCA−CaM complexes correspond to a dissociated autoinhibitory domain, whereas orientationally immobile PMCA−CaM complexes indicate a nondissociated autoinhibitory domain and therefore an inactive enzyme (*28*). The contrast between CaM and CaM_{ox} is accentuated in the presence of ATP. Addition of ATP to complexes of PMCA with native CaM, allowing the enzyme to proceed through its enzymatic cycle, results in a population belonging exclusively to an orientationally mobile state (*28*). In contrast, the present results show that when ATP is added to CaM_{ox} complexes with PMCA, there is still a large fraction of molecules with lower orientational mobility. The decrease in the ability of oxidized CaM to induce dissociation of the autoinhibitory domain from PMCA corresponds with an overall decrease in activity seen in the bulk PMCA activation studies (Figure 1). The results presented here suggest that the inhibition of the PMCA by CaM_{ox} results from the apparent inability of oxidized CaM to induce dissociation of the autoinhibitory domain and thus to invoke sufficient structural change in the autoinhibitory domain of the PMCA to allow for activation.

ACKNOWLEDGMENT

We thank Thomas Squier for helpful discussions. We also thank Jay Unruh for the fluorescence anisotropy measurement of CaM_{ox}-TMR.

REFERENCES

1. Klee, C. B., Crouch, T. H., and Richman, P. G. (1980) Calmodulin, *Annu. Rev. Biochem. 49*, 489−515.
2. Vogel, H. J. (1994) Calmodulin: a Versatile Calcium Mediator Protein, *Biochem. Cell Biol. 72*, 357−376.
3. Van Eldik, L. J., and Watterson, D. M. (1998) *Calmodulin and Signal Transduction*, Academic Press, New York.
4. Weinstein, H., and Mehler, E. L. (1994) Ca^{2+}-Binding and Structural Dynamics in the Functions of Calmodulin, *Annu. Rev. Physiol. 56*, 213−236.
5. Crivici, A., and Ikura, M. (1995) Molecular and Structural Basis of Target Recognition by Calmodulin, *Annu. Rev. Biophys. Biomol. Struct. 24*, 85−116.
6. Carafoli, E. (1997) Plasma Membrane Calcium Pump: Structure, Function and Relationships, *Basic Res. Cardiol. 92*, 59−61.
7. Enyedi, A., Vorherr, T., James, P., McCormick, D. J., Filoteo, A. G., Carafoli, E., and Penniston, J. T. (1989) The Calmodulin Binding Domain of the Plasma Membrane Ca^{2+} Pump Interacts both with Calmodulin and with Another Part of the Pump, *J. Biol. Chem. 264*, 12313−12321.
8. Verma, A. K., Enyedi, A., Filoteo, A. G., and Penniston, J. T. (1994) Regulatory Region of Plasma Membrane Ca^{2+} Pump. 28 Residues Suffice to Bind Calmodulin but More are Needed for Full Auto-Inhibition of the Activity, *J. Biol. Chem. 269*, 1687−1691.
9. Falchetto, R., Vorherr, T., Brunner, J., and Carafoli, E. (1991) The Plasma Membrane Ca^{2+} Pump Contains a Site That Interacts with Its Calmodulin-Binding Domain, *J. Biol. Chem. 266*, 2930−2936.
10. Padanyi, R., Paszty, K., Penheiter, A. R., Filoteo, A. G., Penniston, J. T., and Enyedi, A. (2003) Intramolecular interactions of the regulatory region with the catalytic core in the plasma membrane calcium pump, *J. Biol. Chem. 278*, 35798−35804.
11. Squier, T. C., and Bigelow, D. J. (2000) Protein Oxidation and Age-Dependent Alterations in Calcium Homeostasis, *Front. Biosci. 5*, d504−d526.
12. Gao, J., Yao, Y., Williams, T. D., and Squier, T. C. (1998) Progressive Decline in the Ability of Calmodulin Isolated from Aged Brain To Activate the Plasma Membrane Ca-ATPase, *Biochemistry 37*, 9536−9548.
13. Yao, Y., Yin, D., Jas, G. S., Kuczera, K., Williams, T. D., Schöneich, C., and Squier, T. C. (1996) Oxidative Modification of a Carboxyl-Terminal Methionine in Calmodulin By Hydrogen Peroxide Inhibits Calmodulin-Dependent Activation of the Plasma Membrane Ca-ATPase, *Biochemistry 35*, 2767−2787.
14. Gao, J., Yao, Y., and Squier, T. C. (2001) Oxidatively Modified Calmodulin Binds to the Plasma Membrane Ca-ATPase in a Nonproductive and Conformationally Disordered Complex, *Biophys. J. 80*, 1791−1801.
15. Sun, H., Gao, J., Ferrington, D. A., Biesiada, H., Williams, T. D., and Squier, T. C. (1999) Repair of Oxidized Calmodulin by Methionine Sulfoxide Reductase Restores Ability to Activate the Plasma Membrane Ca-ATPase, *Biochemistry 38*, 105−112.
16. Xie, X. S., and Trautman, J. K. (1998) Optical Studies of Single Molecules at Room Temperature, *Annu. Rev. Phys. Chem. 49*, 441−480.
17. Lu, H. P., Xun, L., and Xie, X. S. (1998) Single-Molecule Enzymatic Dynamics, *Science 282*, 1877−1882.
18. Moerner, W. E., and Orrit, M. (1999) Illuminating Single Molecules in Condensed Matter, *Science 283*, 1670−1676.
19. Weiss, S. (1999) Fluorescence Spectroscopy of Single Biomolecules, *Science 283*, 1676−1683.
20. Weiss, S. (2000) Measuring Conformational Dynamics of Biomolecules by Single Molecule Fluorescence Spectroscopy, *Nat. Struct. Biol. 7*, 724−729.

21. Xie, X. S., and Dunn, R. C. (1994) Probing Single Molecule Dynamics, *Science 265*, 361−364.
22. Ha, T., Laurence, T. A., Chemla, D. S., and Weiss, S. (1999) Polarization Spectroscopy of Single Fluorescent Molecules, *J. Phys. Chem. B 103*, 6839−6850.
23. Warshaw, D. M., Hayes, E., Gaffney, D., Lauzon, A. M., Wu, J., Kennedy, G., Trybus, K., Lowey, S., and Berger, C. (1998) Myosin Conformational States Determined by Single Fluorophore Polarization, *Proc. Natl. Acad. Sci. U.S.A. 95*, 8034−8039.
24. Adachi, K., Yasuda, R., Noji, H., Itoh, H., Harada, Y., Yoshida, M., and Kinosita, K., Jr. (2000) Stepping Rotation of F1-ATPase Visualized Through Angle-resolved Single-fluorophore Imaging, *Proc. Natl. Acad. Sci. U.S.A. 97*, 7243−7247.
25. Sosa, H., Peterman, E. J., Moerner, W. E., and Goldstein, L. S. (2001) ADP-Induced Rocking of the Kinesin Motor Domain Revealed by Single-molecule Fluorescence Polarization Microscopy, *Nat. Struct. Biol. 8*, 540−544.
26. Forkey, J. N., Quinlan, M. E., Shaw, M. A., Corrie, J. E., and Goldman, Y. E. (2003) Three-dimensional Structural Dynamics of Myosin V by Single-molecule Fluorescence Polarization, *Nature 422*, 399−404.
27. Osborn, K. D., Singh, M. K., Urbauer, R. J. B., and Johnson, C. K. (2003) Maximum Likelihood Approach to Single-Molecule Polarization Modulation Analysis, *ChemPhysChem. 4*, 1005−1011.
28. Osborn, K. D., Zaidi, A., Mandal, A., Urbauer, R. J. B., and Johnson, C. K. (2004) Single-Molecule Dynamics of the Calcium-Dependent Activation of Plasma-Membrane Ca^{2+}-ATPase by Calmodulin, *Biophys. J. 87*, 1892−1899.
29. Fabiato, A. (1988) Computer Programs For Calculating Total From Specified Free Or Free From Specified Total Ionic Concentrations In Aqueous Solutions Containing Multiple Metals And Ligands, *Methods Enzymol. 157*, 378−417.
30. Allen, M. W., Urbauer, R. J. B., Zaidi, A., Williams, T. D., Urbauer, J. L., and Johnson, C. K. (2004) Fluorescence Labeling, Purification and Immobilization of a Double Cysteine Mutant Calmodulin Fusion Protein for Single-Molecule Experiments, *Anal. Biochem. 325*, 273−284.
31. Bartlett, R. K., Bieber Urbauer, R. J., Anbanandam, A., Smallwood, H. S., Urbauer, J. L., and Squier, T. C. (2003) Oxidation of Met144 and Met145 in Calmodulin Blocks Calmodulin Dependent Activation of the Plasma Membrane Ca-ATPase, *Biochemistry 42*, 3231−3238.
32. Niggli, V., Adunyah, E. S., Penniston, J. T., and Carafoli, E. (1981) Purified (Ca^{2+}-Mg^{2+})-ATPase of the Erythrocyte Membrane. Reconstitution and Effect of Calmodulin and Phospholipids, *J. Biol. Chem. 256*, 395−401.
33. Niggli, V., Penniston, J. T., and Carafoli, E. (1979) Purification of the (Ca^{2+}-Mg^{2+})-ATPase from Human Erythrocyte Membranes Using a Calmodulin Affinity Column, *J. Biol. Chem. 254*, 9955−9958.
34. Lanzetta, P. A., Alverez, L. J., Reinsch, P. S., and Candia, O. (1979) An Improved Assay for Nanomole Amounts of Inorganic Phosphate, *Anal. Biochem. 100*, 95−97.
35. Majima, E., Gogo, S., Hori, H., Shinohara, Y., Hong, Y.-M., and Terada, H. (1995) Stabilities of the Fluorescent SH-Reagent Eosin-5-Maleimide and its Adducts with Sulhydryl Compounds, *Biochim. Biophys. Acta 1243*, 336−342.
36. Orrenius, S., Burkitt, M. J., Kass, G. E., Dypbukt, J. M., and Nicotera, P. (1992) Calcium Ions and Oxidative Cell Injury, *Ann. Neurol. 32*, S33−S42.
37. Hoyal, C. R., Thomas, A. P., and Forman, H. J. (1996) Hydroperoxide-Induced Increases in Intracellular Calcium Due to Annexin Vi Translocation and Inactivation of Plasma Membrane Ca^{2+}-Atpase, *J. Biol. Chem. 271*, 29205−29210.
38. Denisova, N. A., Strain, J. G., and Joseph, J. A. (1997) Oxidant Injury in Pc12 Cells-A Possible Model of Calcium "Dysregulation" in Aging: II. Interactions with Membrane Lipids, *J. Neurochem. 69*, 1259−1266.
39. Eu, J. P., Xu, L., Stamler, J. S., and Meissner, G. (1999) Regulation of Ryanodine Receptors by Reactive Nitrogen Species, *Biochem. Pharmacol. 57*, 1079−1084.
40. Guerini, D., Krebs, J., and Carafoli, E. (1984) Stimulation of the Purified Erythrocyte Ca^{2+}-ATPase by Tryptic Fragments of Calmodulin, *J. Biol. Chem. 259*, 15172−15177.
41. Persechini, A., McMillan, K., and Leakey, P. (1994) Activation of Myosin Light Chain Kinase and Nitric Oxide Synthase Activities by Calmodulin Fragments, *J. Biol. Chem. 269*, 16148−16154.
42. Johnson, J. D., Snyder, C., Walsh, M., and Flynn, M. (1996) Effects of Myosin Light Chain Kinase and Peptides on Ca^{2+} Exchange with the N- and C-Terminal Ca^{2+} Binding Sites of Calmodulin, *J. Biol. Chem. 271*, 761−767.
43. Bayley, P. M., Findlay, W. A., and Martin, S. R. (1996) Target Recognition by Calmodulin: Dissecting the Kinetics and Affinity of Interaction Using Short Peptide Sequences, *Protein Sci. 5*, 1215−1228.
44. Barth, A., Martin, S. R., and Bayley, P. M. (1998) Specificity and Symmetry in the Interaction of Calmodulin Domains with the Skeletal Muscle Myosin Light Chain Kinase Target Sequence, *J. Biol. Chem. 273*, 2174−2183.
45. Sun, H., and Squier, T. C. (2000) Ordered and Cooperative Binding of Opposing Globular Domains of Calmodulin to the Plasma Membrane Ca-ATPase, *J. Biol. Chem. 275*, 1731−1738.
46. Yao, Y., Gao, J., and Squier, T. C. (1996) Dynamic Structure of the Calmodulin-Binding Domain of the Plasma Membrane Ca-ATPase in Native Erythrocyte Ghost Membranes, *Biochemistry 35*, 12015−12028.
47. Toyoshima, C., Nakasako, M., Nomura, H., and Ogawa, H. (2000) Crystal Structure of the Calcium Pump of Sarcoplasmic Reticulum at 2.6 Å Resolution, *Nature 405*, 647−655.
48. Toyoshima, C., and Nomura, H. (2002) Structural Changes in the Calcium Pump Accompanying the Dissociation of Calcium, *Nature 418*, 605−611.
49. Xu, C., Rice, W. J., He, W., and Stokes, D. L. (2002) A Structural Model for the Catalytic Cycle of Ca^{2+}-ATPase, *J. Mol. Biol. 316*, 201−211.
50. O'Neil, K. T., Wolfe, H. R., Erickson-Viitanen, S., and DeGrado, W. E. (1987) Fluorescence Properties of Calmodulin-Binding Peptides Reflect Alpha-Helical Periodicity, *Science 236*, 1454−1457.
51. Roth, S. M., Schneider, D. M., Strobel, L. A., VanBerkum, M. F. A., Means, A. R., and Wand, A. J. (1991) Structure of the Smooth Muscle Myosin Light-Chain Kinase Calmodulin-Binding Domain Peptide Bound to Calmodulin, *Biochemistry 30*, 10078−10084.
52. Ikura, M., Clore, G. M., Gronenborn, A. M., Zhu, G., Klee, C. B., and Bax, A. (1992) Solution Structure of a Calmodulin-Target Peptide Complex by Multidimensional NMR, *Science 256*, 632−638.
53. Meador, W. E., Means, A. R., and Quiocho, F. A. (1992) Target Enzyme Recognition by Calmodulin: 2.4 Å Structure of a Calmodulin-Peptide Complex, *Science 257*, 1251−1255.
54. Zhang, M., and Vogel, H. J. (1994) The Calmodulin-Binding Domain of Caldesmon Binds to Calmodulin in an α-Helical Conformation, *Biochemistry 33*, 1163−1171.
55. O'Neil, K. T., and DeGrado, W. F. (1990) How Calmodulin Binds its Targets: Sequence Independent Recognition of Amphiphilic Alpha-Helices, *Trends Biochem. Sci. 15*, 59−64.
56. LaPorte, D. C., Wierman, B. M., and Storm, D. R. (1980) Calcium-Induced Exposure of a Hydrophobic Surface on Calmodulin, *Biochemistry 19*, 3814−3819.
57. Nelson, M. R., and Chazin, W. J. (1998) An Interaction-Based Analysis of Calcium-Induced Conformational Changes in Ca^{2+} Sensor Proteins, *Protein Sci. 7*, 270−282.
58. Edwards, R. A., Walsh, M. P., Sutherland, C., and Vogel, H. J. (1998) Activation of Calcineurin and Smooth Muscle Myosin Light Chain Kinase by Met-to-Leu Mutants of Calmodulin, *Biochem. J. 331*, 149−152.
59. Jas, G. S., and Kuczera, K. (2002) Free-Energy Simulations of the Oxidation of C-Terminal Methionines in Calmodulin, *Proteins: Struct., Funct., Genet. 48*, 257−268.
60. Yin, D., Sun, H., Weaver, R. F., and Squier, T. C. (1999) Nonessential Role for Methionines in the Productive Association Between Calmodulin and the Plasma Membrane Ca-ATPase, *Biochemistry 38*, 13654−13660.

BI048806P